Journal of Molecular Structure 1006 (2011) 684–691

Contents lists available at SciVerse ScienceDirect

Journal of Molecular Structure

journal homepage: www.elsevier.com/locate/molstruc

# The new sulphur-containing ligand 4′-(4-methylthiophenyl)-3,2′:6′,3″-terpyridine (**L1**) and the supramolecular structure of the dinuclear complex $[Zn_2(\mu\text{-}\mathbf{L1})(acac)_4]$ (acac = acetylacetonato): The key role of non-covalent S···O contacts and C–H···S hydrogen bonds

Juan Granifo [a,*], Rubén Gaviño [b], Eleonora Freire [c,d,1], Ricardo Baggio [c]

[a] Departamento de Ciencias Químicas y Recursos Naturales, Facultad de Ingeniería, Ciencias y Administración, Universidad de La Frontera, Casilla 54-D, Temuco, Chile
[b] Instituto de Química, Universidad Nacional Autónoma de México, Cd. Universitaria, Circuito Exterior Coyoacán, 04510 México, DF, Mexico
[c] Departamento de Física, Comisión Nacional de Energía Atómica, Av. Gral Paz 1499, 1650 San Martín, Pcia. de Buenos Aires, Argentina
[d] Escuela de Ciencia y Tecnología, Universidad Nacional de San Martín, Buenos Aires, Argentina

ARTICLE INFO

*Article history:*
Received 21 August 2011
Received in revised form 19 October 2011
Accepted 20 October 2011
Available online 28 October 2011

*Keywords:*
S···O interactions
C–H···S hydrogen bonds
Zinc(II) complexes
Acetylacetonate
4′-(4-Methylthiophenyl)-3,2′:6′,3″-terpyridine

ABSTRACT

The new terpyridyl ligand 4′-(4-methylthiophenyl)-3,2′:6′,3″-terpyridine (**L1**) combines with $Zn(acac)_2$ to form the dizinc complex $[Zn_2(\mu\text{-}\mathbf{L1})(acac)_4]$ (**1**) (acac = acetylacetonato). The single crystal structure of **1** shows the existence of two different $Zn(acac)_2$ centres bridged by the **L1** ligand through its two 3-pyridyl-nitrogen atoms. The acac and **L1** ligands allow the generation of a series of intra- and intermolecular hydrogen bonds of the C–H···N, C–H···O and C–H···π type. In addition, the presence of the $CH_3$–S group in **L1** plays a crucial role by providing the non-covalent S···O, S···H and H($CH_3$)···O contacts, which permit to describe fully this unusual supramolecular network. The NMR spectra of **1** in $CDCl_3$ solution confirm the presence of the two zinc atoms joined by the bridging **L1** ligand, but, differently to the solid state, their environments are identical.



## 1. Introduction

The study of the coordination chemistry of 2,2′:6′,2″-terpyridine and its derivatives has been ascribed more widely to its action as chelating ligands, i.e., where they present a convergent disposition of its N-pyridyl donor atoms to link the metal centres [1,2]. In contrast, terpyridine-based ligands with the divergent mode able to bridge at least two metal centres are scarse; a few recent examples can be found mainly for functionalized 4,2′:6′,4″-terpyridines [3]. In this regard and only in two recent works, 3,3″ divergent and 4′-functionalized terpyridines [4′-phenyl-3,2′:6′,3″-terpyridine (**L2**, Scheme 1) and 4′-(4-pyridyl)-3,2′:6′,3″-terpyridine] involving the N 3-pyridyl atoms as linkers have been used [4]. More specifically, the reported examples that include one of these ligands are a coordination polymer [4b] and a dinuclear compound [4a]. This last complex, which incorporates the **L2** ligand, was formulated as $[Zn_2(\mu\text{-}\mathbf{L2})(acac)_4]\cdot H_2O$ (acac = acetylacetonato) (**2**). The supramolecular structure of **2** was described on the basis of the key role played by the acac and **L2** ligands and the guest water molecule by using a series of intermolecular hydrogen bonds: either conventional (of the O–H/O type) or non-conventional (C–H/O and CH/π [5,6]) including those CH/π arising between the coordinated acac ligand and phenyl rings, recently proposed by Zarić et al. [7]. Zarić et al. demonstrated that the chelating acac shows two types of interactions, one by using either its CH and/or $CH_3$ groups (hydrogen bond donor) and the other one involving the π-system of the chelate ring (as a hydrogen bond acceptor). With the aim on going further in the study of the bonding and supramolecular properties of this kind of systems, we replaced the **L2** ligand, with its phenyl ring, by the related **L1** ligand, with a 4-methylthiophenyl group instead (Scheme 1). The result of the reaction of **L1** with $Zn(acac)_2$ was the new dizinc complex $[Zn_2(\mu\text{-}\mathbf{L1})(acac)_4]$ (**1**) with the sulphur atom of the 4-methylthio substituent non-coordinated, but instead it appears involved in the singular non-covalent S···O and S···H interactions.

## 2. Results and discussion

### 2.1. Synthesis

The **L1** ligand was prepared via the one-step general method by mixing 3-acetylpyridine, 4-(methylthio)benzaldehyde and $NH_3$ in

* Corresponding author.
*E-mail address:* jgranifo@ufro.cl (J. Granifo).
[1] Member of CONICET.

0022-2860/$ - see front matter © 2011 Elsevier B.V. All rights reserved.
doi:10.1016/j.molstruc.2011.10.038

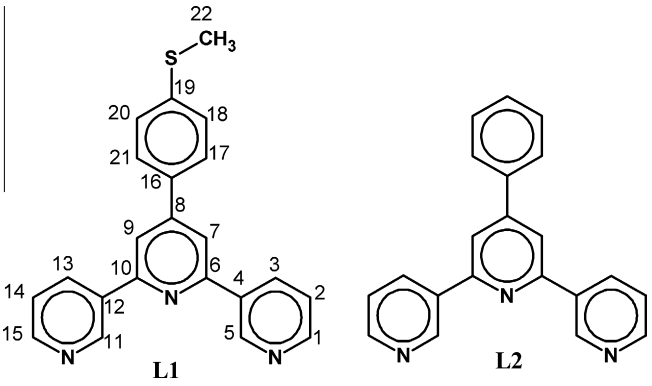


**Scheme 1.** The sketches of the ligands **L1** and **L2**. For **L1** the numbering of carbon atoms (hydrogen atoms where correspond) is indicated.

a EtOH solution. The newly synthesized ligand was characterized by elemental analysis, $^{1}H$, $^{13}C$ and 2D NMR experiments, mass spectrometry and IR spectroscopy. Complex **1** was prepared by the reaction of an excess of $Zn(acac)_2$ with **L1** in a hot acetonitrile solution, from which colourless blocks suitable for single crystal X-ray analysis were obtained.

### 2.2. The NMR spectra of *L1* (performed through COSY, DEPT, PND)

The NMR results in $CDCl_3$ solution of the **L1** molecule are in good agreement with the expected molecular structure (Scheme 1 and Section 5.1). Thus, the $^{13}C$ NMR spectrum shows one solitary methyl group (15.13 (C22) ppm) and the corresponding signals of the aromatic region: four due to quaternary carbons [134.00 (C16 superimposed with C4/C12), 140.76 (C19), 149.69 (C8), 155.00 (C6/C10) ppm] and seven due to CH carbons [116.83 (C7/C9), 123.38 (C2/C14), 126.34 (C17/C21), 127.10 (C18/C20), 134.22 (C3/C13), 148.13 (C1/C15), 149.95 (C5/C11) ppm]. Similarly, the $^{1}H$ NMR is characterized for a high field singlet (2.48 ppm) due to the three protons of the thiomethyl group. The four phenyl protons can be readily distinguished from the other for the characteristic AA′BB′ pattern of H18/H20 (7.30 ppm) and H17/H21 (7.57 ppm). The two protons of the central pyridine ring H7/H9 appear as a sharp singlet (7.79 ppm). Those four protons of the 3-pyridyl groups next to the electronegative N atoms, H5/H11 (9.29 ppm) and H1/H15 (8.63 ppm), together with the two H3/H13 (8.39 ppm) protons, show the largest displacement towards low field. The two remaining protons H2/H14 (7.36 ppm) of the 3-pyridyl rings appear in a predictable manner as a multiplet.

### 2.3. Coordination geometry and bonding in *1*

The crystal and molecular structure of **1** was determined by single crystal X-ray diffraction at 273 K and it consists of a bis-monodentate **L1** ligand bridging the Zn1 and Zn2 atoms from two different $\{Zn(acac)_2\}$ fragments, through its 3-pyridyl N atoms (Fig. 1 and Table 1). Even if crystallizing in the non-centrosymmetric space group Cc, the molecular assembly presents a strongly-pseudo twofold rotation axis in a way that the whole symmetry ends up mimicking the C2/c space group; the whole molecular body abides to this pseudo operation, while the terminal $PhSCH_3$ group, which would not possible respond to this C2 operation, appears disordered into two almost equally populated halves (occupancies: higher, 0.532; lower, 0.468), thus complying with the pseudosymmetry. Refinement in the centrosymmetric space group, however, resulted in much higher R indices, for what a constrained refinement in Cc was preferred, and it is the one herein reported.

Each Zn centre (Zn1/Zn2) has a $NO_4$ coordination sphere; four sites are provided by two different acac groups coordinated in the usual chelating form through their carbonyl O donor, the

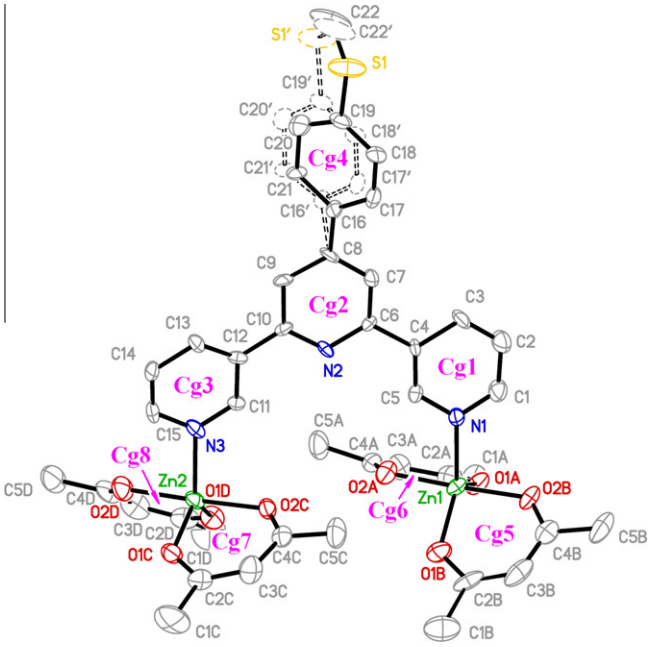


**Fig. 1.** Molecular diagram of **1**, with anisotropic displacement ellipsoids drawn at a 40% probability level. The disordered $PhSCH_3$ end shown in full/broken lines. H atoms removed, for clarity.

**Table 1**
Selected bond lengths (Å) and bond angles (°) for **1**.

| | |
|---|---|
| *Bond distances* | |
| Zn1–O1A | 1.948(3) |
| Zn1–O1B | 1.986(3) |
| Zn1–O2A | 2.009(4) |
| Zn1–O2B | 2.061(4) |
| Zn1–N1 | 2.091(2) |
| Zn2–O1C | 2.010(3) |
| Zn2–O1D | 1.941(3) |
| Zn2–O2C | 2.055(4) |
| Zn2–O2D | 2.067(4) |
| Zn2–N3 | 2.099(3) |
| *Bond angles* | |
| O1A–Zn1–O1B | 119.19(14) |
| O1A–Zn1–O2A | 90.15(14) |
| O1B–Zn1–O2A | 92.95(15) |
| O1A–Zn1–O2B | 88.97(14) |
| O1B–Zn1–O2B | 89.54(15) |
| O2A–Zn1–O2B | 177.49(14) |
| O1A–Zn1–N1 | 112.84(12) |
| O1B–Zn1–N1 | 127.96(13) |
| O2A–Zn1–N1 | 87.36(13) |
| O2B–Zn1–N1 | 90.81(12) |
| O1C–Zn2–O1D | 119.57(14) |
| O1C–Zn2–O2C | 91.43(14) |
| O1D–Zn2–O2C | 91.31(14) |
| O1C–Zn2–O2D | 90.15(15) |
| O1D–Zn2–O2D | 89.09(16) |
| O2C–Zn2–O2D | 177.91(13) |
| O1C–Zn2–N3 | 113.27(12) |
| O1D–Zn2–N3 | 127.15(13) |
| O2C–Zn2–N3 | 88.64(13) |
| O2D–Zn2–N3 | 89.49(14) |

planar groups subtending to each other angles of 61.6/60.2° for Zn1/Zn2, respectively. The fifth site of the coordination polyhedron is occupied by a 3-pyridyl N atom from the **L1** ligand. The geometry around each Zn atom is an almost perfect trigonal bipyramid, with apical O2A–Zn1–O2B/O2C–Zn2–O2D angles of 177.5/177.9° and the apical bonds deviating by less than 1.9/0.9° from the normal

to the equatorial base. The pyridine-based rings of the **L1** ligand depart somewhat from a nearly planar structure; each outer pyridyl group is twisted with respect to the central one, subtending dihedral angles of 10.9/10.0° to this ring and 15.3° to each other. The two disordered images of the terminal phenyl groups appear almost at 180° from one another, and form dihedral angles of 39.0/44.4° to the central pyridyl ring.

### 2.4. Solid state weak interactions in *1*

Compound **1** is very similar to its recently published dinuclear $[Zn_2(\mu\text{-}\mathbf{L2})(acac)_4]\cdot H_2O$ **(2)** analogue (**L2** = 4′-phenyl-3,2′:6′,3″-terpyridine, Scheme 1) [4a]. The similarities between **1** and **2** reflect also in the packing disposition although **1** lacks the hydration water molecule, which is responsible in **2** of the generation of strongly coupled hydrogen bonded units into a 1D chain along b (Scheme 2). Notably, in **1** the water site is occupied by the $-SCH_3$ group, which fulfils the function of accomplishing a 1D chain of non-covalent intermolecular interactions. Both one-dimensional structures present similar, though differently connected, interlinked CH/O and CH/π contacts to go then into a 2D array. These planar structures are further linked by a large number of CH/π contacts in a final 3D network.

#### 2.4.1. Intramolecular interactions in *1*

Fig. 2 shows the intramolecular interactions present in **1**. The three pyridine-based rings are internally connected by two hydrogen bonds involving the bifurcated N lone pairs on the central terpyridine ring and the H atoms of the lateral 3-pyridyl groups, H5···N2 [C5···N2, 2.836 Å, 103°] and H11···N2 [C11···N2, 2.833 Å, 100°], something which has been observed in a number of similar systems [8]. This 2D structure is further connected to the apical acac oxygen atoms through four CH(3-pyridyl)···O contacts H1···O2B [C1···O2B, 3.022 Å, 117°], H5···O2A [C5···O2A, 3.037 Å, 108°], H11···O2C [C11···O2C, 2.992 Å, 109°] and H15···O2D [C15···O2D, 3.022 Å, 117°], whose geometric parameters are compatible with this type of links [6].

#### 2.4.2. 1D supramolecular structure of *1*: relevance of the S···O and S···H interactions

The directional tendency of the S···X interactions including the S···H and S···O for the divalent sulphur atom have been evaluated by Rosenfield et al. [9]. The interactions were characterized by two types of surrounding environments for the sulphur atom relative to the C–S–C plane (Scheme 3). Type I are electrophiles which tend to interact over and under the plane with the sulphur lone-pair of

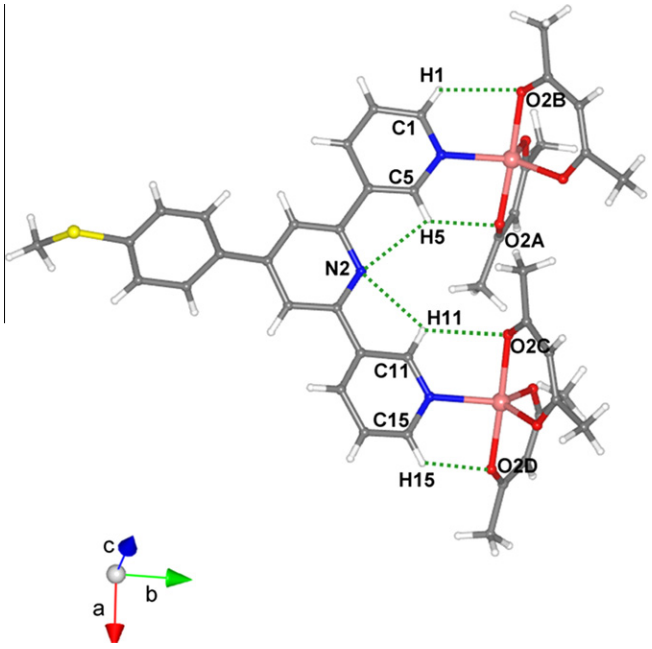


**Fig. 2.** N···H and O···H intramolecular hydrogen bonding in **1** (only the higher occupancy conformer is shown).

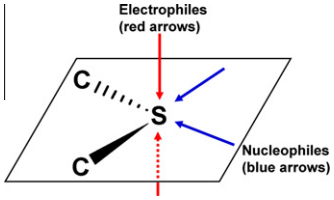


**Scheme 3.** Directionality of nucleophiles and electrophiles towards the sulphur atom in non-covalent S···X interactions. (For interpretation of the references to colour in this artwork, the reader is referred to the web version of this article.)

the highest occupied molecular orbital (HOMO). Type II are nucleophiles that approach the sulphur backwards with directions close to those of the S–C bonds, providing electrons to the antibonding lowest unoccupied molecular orbital (LUMO) of the S–C bonds. Later, the specific intermolecular S···O and S···H distances were evaluated by Iwaoka et al. [10] and van den Berg and Seddon [11] through comprehensive data base studies, which showed that the highest

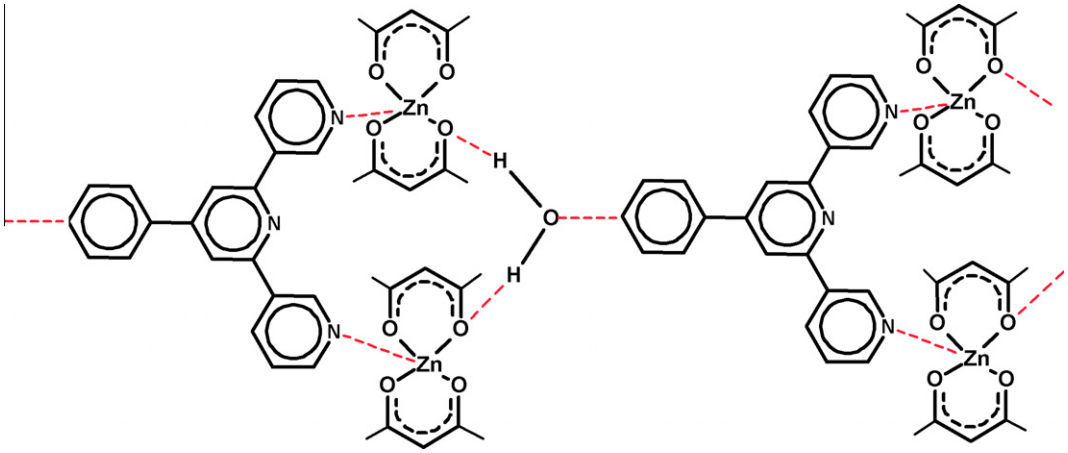


**Scheme 2.** The 1D chain running along b in the complex **2**.

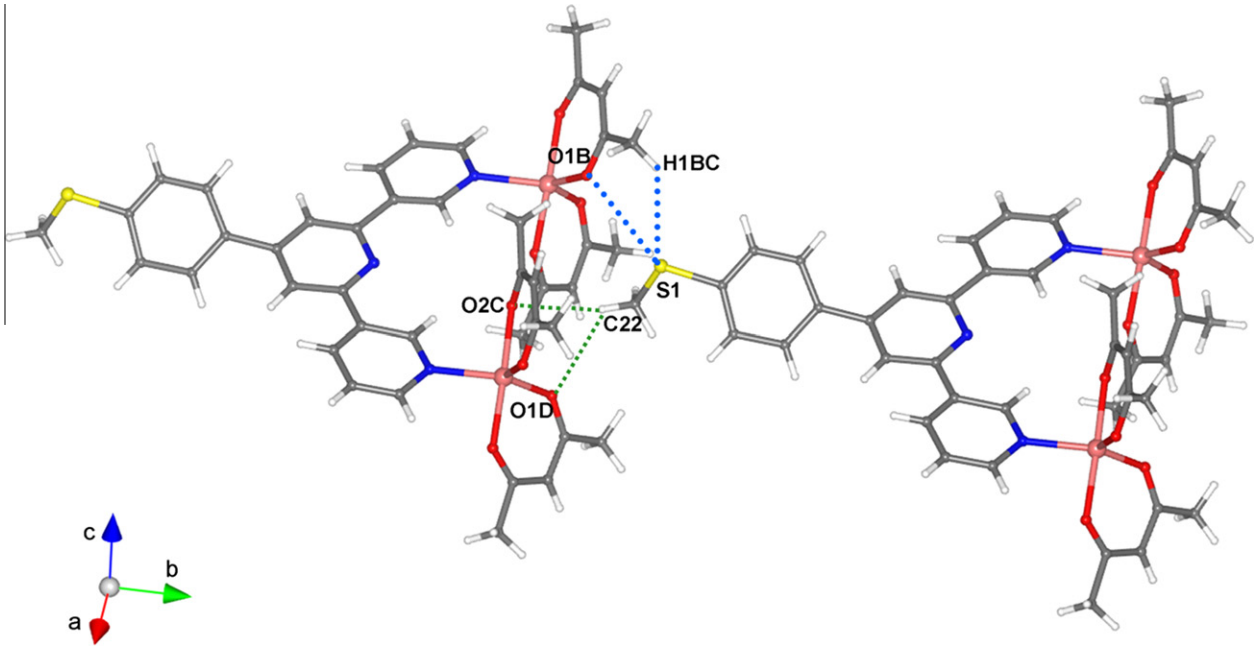


**Fig. 3.** Non-covalent interactions (1D supramolecular structure) in the higher occupancy conformation of **1**: blue dotted lines involve the sulphur atom; green broken lines involve the thiomethyl H-atoms. (For interpretation of the references to colour in this figure legend, the reader is referred to the web version of this article.)

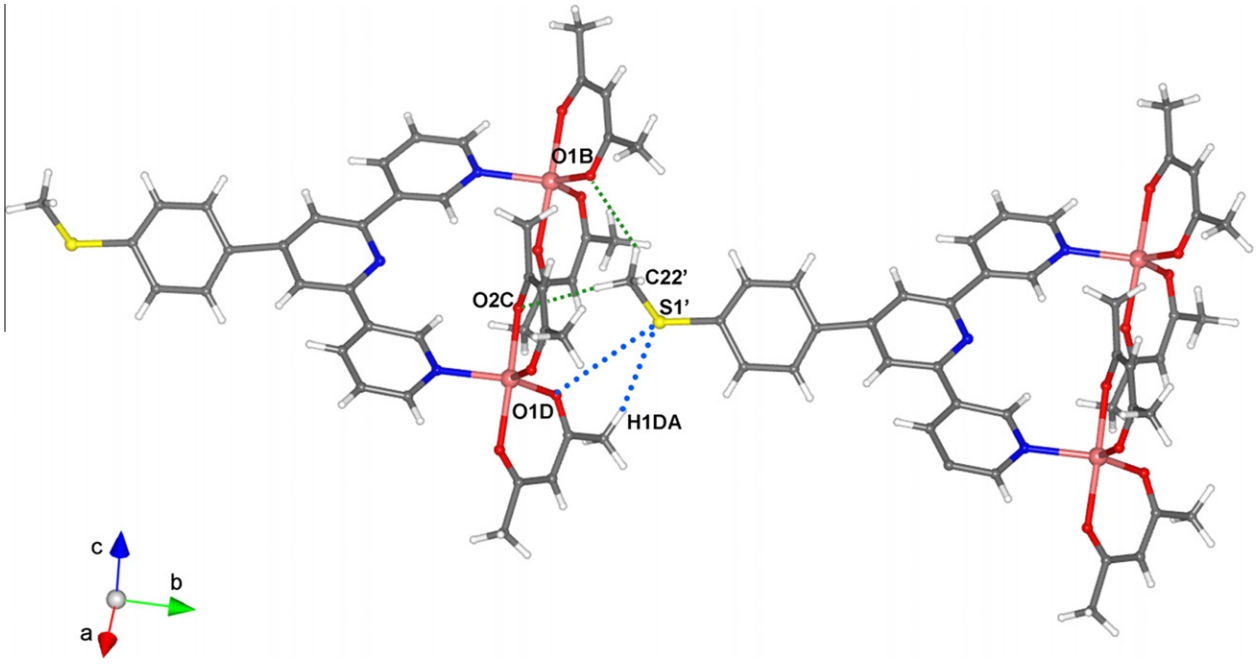


**Fig. 4.** Non-covalent interactions (1D supramolecular structure) in the lower occupancy conformation of **1**: blue dotted lines involve the sulphur atom; green broken lines involve the thiomethyl H-atoms. (For interpretation of the references to colour in this figure legend, the reader is referred to the web version of this article.)

incidence values were centred at 3.82 and 3.21 Å, respectively. In **1** the two orientations due to the disordered $PhSCH_3$ groups display similar S···O and S···H interactions (Figs. 3 and 4). Thus, the S···O distances are very close (S1···O1B, 3.651 Å; S1′···O1D, 3.710 Å), but a little shorter than the expected value (3.82 Å) for this kind of interactions [10]. The geometry of these contacts resembles Type II interaction ones: the O atoms are located close to the plane of the C–S–C unit and the interaction can be conceived as the donation of lone pair electrons located on the oxygen atoms towards the empty $\sigma^*$ orbital of the S–C bonds. Likewise, the geometry of the interaction between the C–H (acac-methyl) with the sulphur atom can be assigned as a Type I contact, where the role of the sulphur atom is to act as an electron donor. S···H distances are almost equal (S1···H1BC, 2.769 Å; S1′···H1DA, 2.779 Å) and significantly shorter than the "highest incidence" value (3.21 Å) [11]. A similar coexistence of the interactions of Type I (C–H···S) and Type II (S···O) has been reported previously for an aromatic disulphide [12].

In addition to the above sulphur-based interactions, two C–H(thiomethyl)···O(acac) hydrogen bonds are present in both disordered structures to reinforce the 1D chains (Figs. 3 and 4). The C···O bond distances and angles of these CH/O links [higher occupancy conformer: C22···O2C, 3.899 Å, 161°; C22···O1D, 3.602 Å,

132°; lower occupancy conformer: C22′···O2C, 3.434 Å, 153°; C22′···O1B, 3.387 Å, 140°] show features to be expected when weaker C–H donor species are involved, such as $CH_3$ groups [6]. In this particular case, in support of this H-donor capacity of the methyl groups, solution NMR studies [13] have evidenced that they are engaged in intermolecular interactions when linked to divalent sulphur atoms, i.e., the acidity of the methyl protons is increased by this kind of link.

*2.4.3. 2D supramolecular structure of **1**: based on CH/O and CH/π hydrogen bonds*

The above one-dimensional H-bonded chains are then put together side by side generating 2D structures through an assembly of CH/O and CH/π hydrogen bonds: six CH(pyridyl)/O(acac), two CH(pyridyl)/π(phenyl ring) and two CH(pyridyl)/π(chelate-acac ring) (Fig. 5). Four of the CH(pyridyl)/O(acac) contacts, envisaged as significant since their C···O distances are in the range 3.470–3.628 Å [6b], are provided by two bifurcated CH donor groups (C7H7 and C9H9). The two remaining CH(pyridyl)/O(acac) connections, with short C···O distances (3.206 and 3.208 Å), are also carried out by bifurcated hydrogen bonds, but only via their mayor components (C3H3···O1C and C13H13···O1A). In spite of this, the bond distances and mainly the magnitude of the angles (>130°) of all these CH/O connections [C7···O1C, 3.628 Å, 161°; C7···O2D, 3.560 Å, 136°; C9···O1A, 3.606 Å, 163°; C9···O2B, 3.470 Å, 134°; C3···O1C, 3.206 Å, 135°; C13···O1A, 3.208 Å, 137°] allow to infer the existence of this type of interactions [6]. The following two interactions are of the CH(pyridyl)/π(phenyl ring) type, now including the π system of the disordered phenyl rings (two interactions on each disordered ring). These interactions in **1** agree with the correlations established previously by Nishio et al. [5], by using as a parameter the short distance H(donor)···C(acceptor) when the interacting groups are aromatic (average value 2.90 ± 0.13 Å). More specifically, in **1** these contacts correspond to H1···C20 (H1···C20′) and H15···C18 (H15···C18′) with a H···C distances of 2.794 (3.026) and 2.941 (2.872) Å, respectively (Fig. 5). The two final synthons that complete the 2D structure are unusual: they include the acetylacetonate ligand in CH/π interactions, CH(pyridyl)/π(chelate-acac ring), which have been revealed recently by Zarić et al. [7]. In this particular case, the H-donor groups CH(pyridyl) correspond to the above mentioned bifurcated H-bonds (C3–H3 and C13–H13) via their minor components, which interact with the π electrons of the acetylacetonato chelate rings (Fig. 5). In this situation, the H···Cg(centroid of the

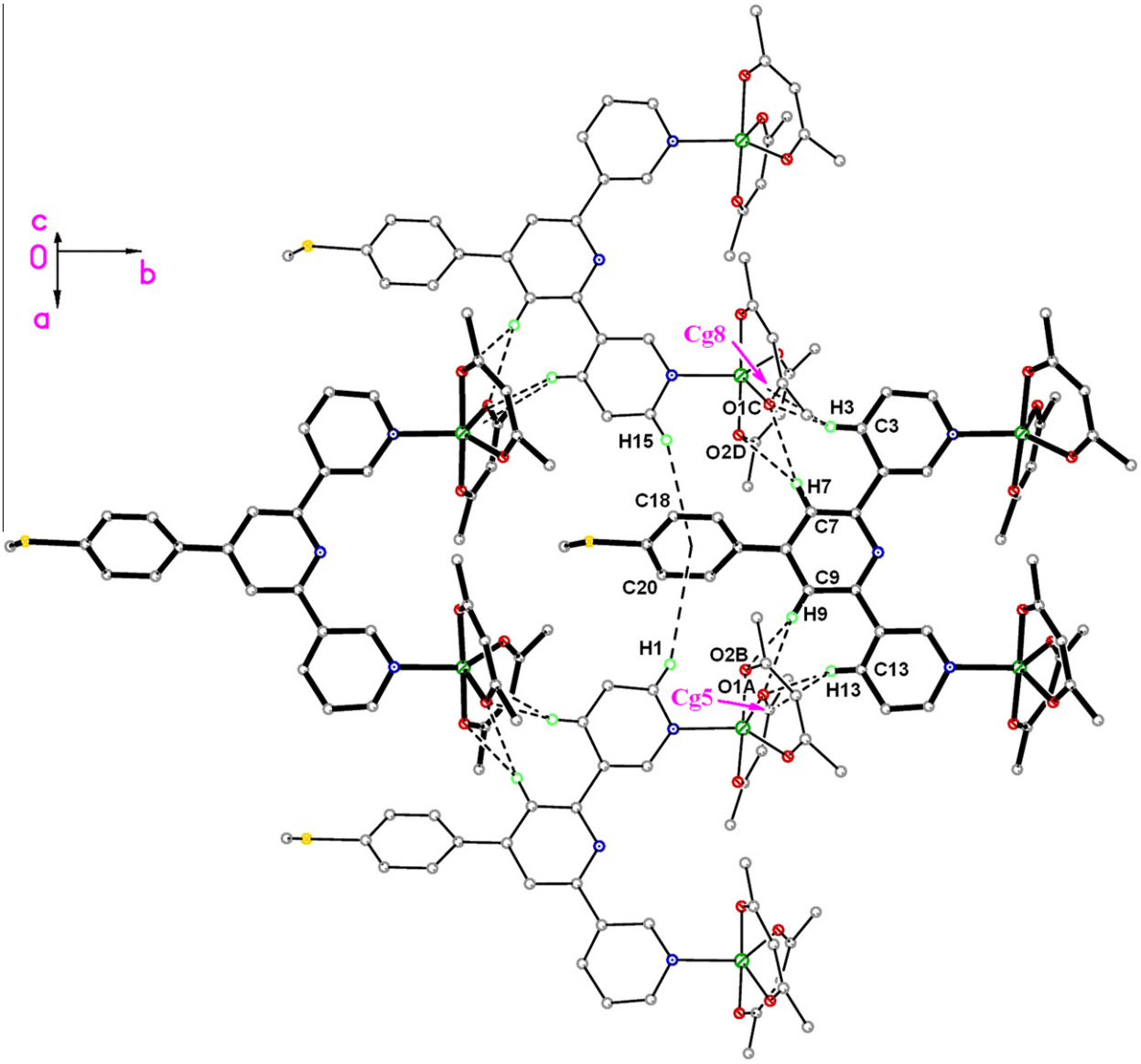


**Fig. 5.** Non-covalent interactions (2D supramolecular structure) in the higher occupancy conformation of **1**.

acetylacetonate ring) distances are used to define the linkages. The H3···Cg8 and H13···Cg5 distances of 2.785 and 2.871 Å in **1** correlate well with the expected range (2.45–3.44 Å) for complexes containing borderline Lewis acid metals such as the Zn(II) cation [7].

*2.4.4. 3D supramolecular structure of **1**: based on CH/π hydrogen bonds*

To form the final 3D structure the above described 2D layers are stacked involving the acetylacetonate ligand either as H-donor and/or H-acceptor in CH/π interactions (Figs. 6 and 7). It is possible to observe ten of this kind of contacts which can be classified in two classes. The first class include the acetylacetonate ligand (CH and $CH_3$) as H-donor in six interactions with the terpyridine-base pyridyl groups as H-acceptors (Fig. 6). Inside this class, the CH groups are involved in four contacts [H3D···Cg3, 3.229 Å; H3C···Cg3, 3.356 Å; H3A···Cg1, 3.320 Å; H3B···Cg1, 3.315 Å] and the $CH_3$ groups in two contacts [H1BB···Cg2, 2.932 Å; H1DC···Cg2, 3.126 Å], with H···Cg bond lengths clearly centred within the observed ranges for complexes with metal-ion of borderline hardness, 2.84–3.45 Å and 2.7–3.5 Å, respectively [7]. In the second class of CH/π interactions appear four equivalent links that involve exclusively the acetylacetonato ligands (Fig. 7). More specifically, the $CH_3$ groups act as H-donors and the chelate rings as H-acceptors [H5AC···Cg5, 3.390 Å; H5CC···Cg8, 3.142 Å; H5DC···Cg7, 3.170; H5BC···Cg6, 3.272 Å]. In a previous work [4a], the range of the distances in what occur these H($CH_3$)···Cg(acac-chelate) interactions have been considered similar to those of the H($CH_3$)···Cg(pyridyl) interactions. Therefore, since these interaction in **1** (3.142–3.339 Å) fall inside of the expected range as indicated above (2.7–3.5 Å) [7], it seems acceptable to postulate the presence of this kind of weak interactions.

*2.4.5. The cell size*

As already stated, compounds **1** and **2** present similar structures with the sole difference that the –$SCH_3$ group plays in **1** the role of an intermolecular bridge which the water molecule fulfils in **2**. But as a result the molecules are differently connected through their non-covalent bonds. An interesting observation is that these clear differences in non-covalent interactions in both structures readily explain some differences found in cell parameters. For example, when comparing **2** with **1** a cell contraction along **b** is observed (17.2414(13) Å in **2** vs. 16.8640(5) Å in **1**) as well as an expansion along **a** and **c** (16.9967(13) and 14.2974(11) Å vs. 17.7602(7) and 14.5089(5) Å). Here, the most significant difference occurs along **a** (0.7635 Å). This effect can be attributed, in part, to the strong O···H interactions of the water molecule that bridge the two Zn(acac)$_2$ fragments in **2** getting them closer (Scheme 2). As an experimental support to this argument are the distances between the Zn(II) centres which reside in the (0 0 1) plane: the one in **2** (6.7509(7) Å) is revealingly shorter than that in **1** (7.1077(4) Å). So, the expansion of **1** in the (0 0 1) plane indeed could be understood as a contraction of **2** in this plane.

## 3. Structure of 1 in solution. A nuclear magnetic resonance study

The diamagnetic compound **1** is soluble in $CHCl_3$ where it was characterized by mono- and two dimensional NMR ($^1$H and $^{13}$C) at room temperature (Section 5.2). The analysis of the results evidenced that the complex **1** has the Zn1/Zn2 metal centres in magnetically equivalent environments. Consequently, the asymmetric molecular structure in the solid state switches to a symmetric one in solution. In this way, the $^{13}$C spectrum show a pattern similar to that of the free ligand **L1** (Sections 2.2 and 5.2) with three additional signals provide by the four equivalent chelating acac ligands [28.26 ppm (8 C, methyl groups); 100.01 ppm (4 C, methine groups); 193.67 ppm (8 C, acetyl groups)]. Likewise, the proton spectrum contains the signals corresponding to ligand **L1** (atom numbering in Scheme 1) symmetrically coordinated [2.57 ppm (S–$CH_3$); 7.40 ppm (H18/H20); 7.57 ppm (H2/H14); 7.66 ppm (H17/H21); 7.94 ppm (H7/H9); 8.65 ppm (H1/H15); 8.68 ppm (H3/H13); 9.32 ppm (H5/H11)] plus two singlets supplied by the acetylacetonate ligands [2.04 ppm (methyl groups, 24 H); 5.40 ppm (methine groups, 4 H)].

An additional feature emerges by comparing the proton signals of the coordinated **L1** with respect to when it is free. The proton

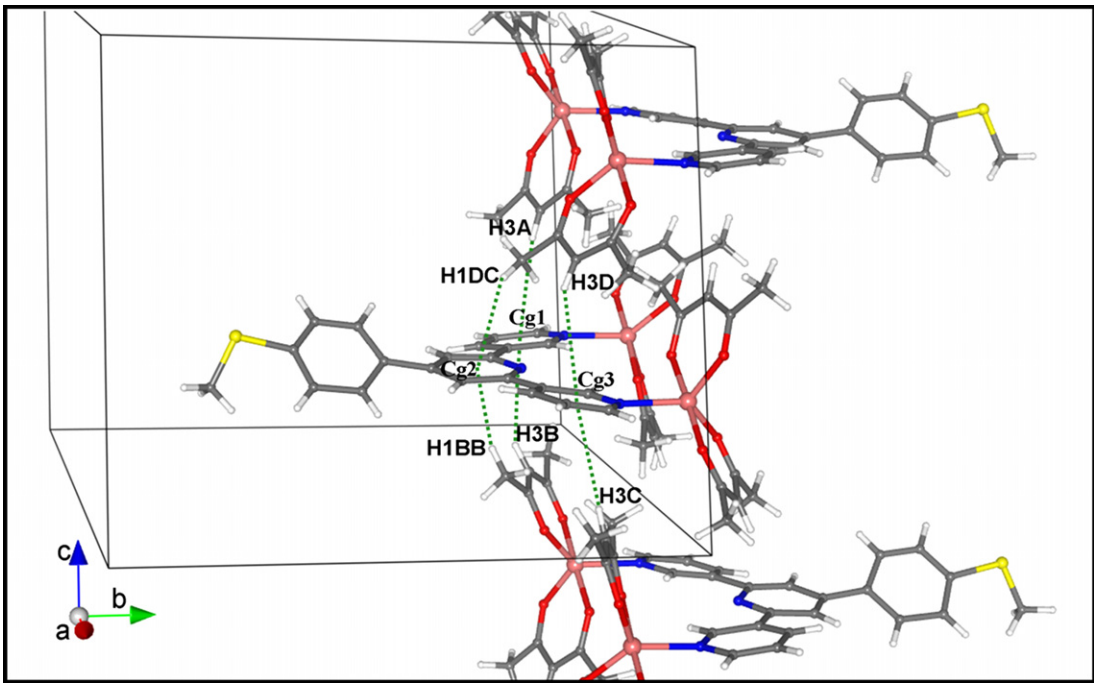


**Fig. 6.** CH/π hydrogen bonds (3D supramolecular structure) in the stacking of **1** involving the acac CH and $CH_3$ groups as H-donor towards the three pyridyl rings (only the higher occupancy conformer is shown).

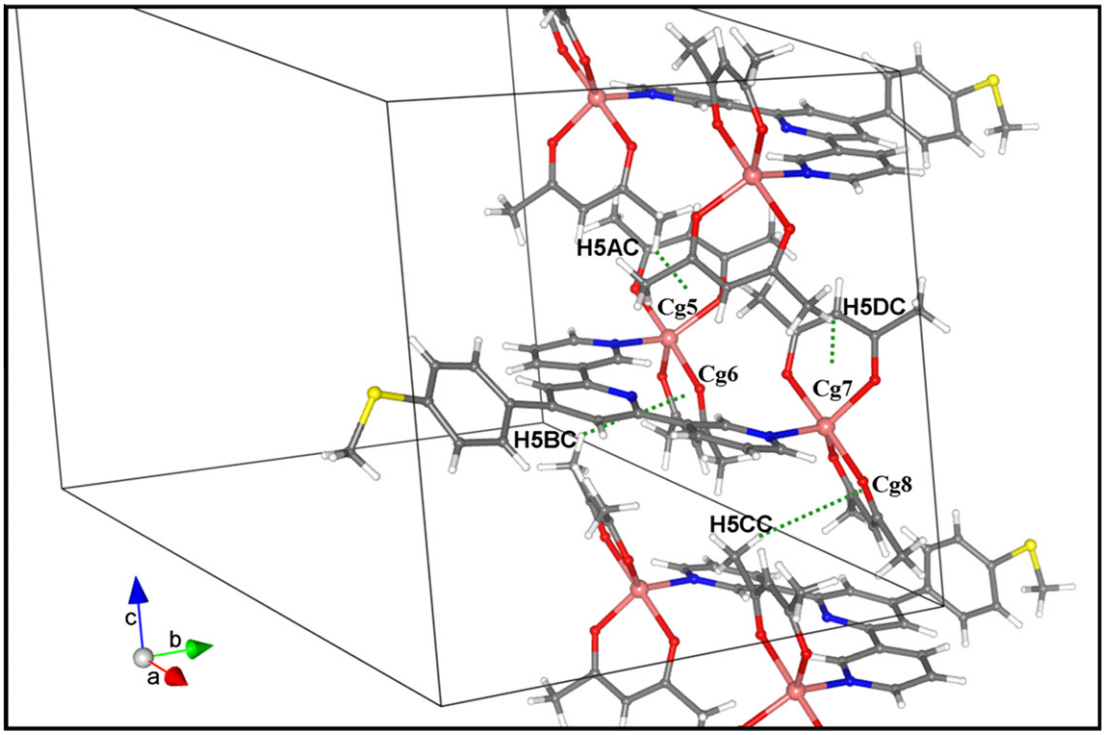


**Fig. 7.** CH/π hydrogen bonds (3D supramolecular structure) in **1** implicating only the acac ligand: the $CH_3$ groups act as H-donors and the chelate rings as H-acceptors (only the higher occupancy conformer is shown).

**Table 2**
Crystal data and refinement parameters of **1**.

| | |
|---|---|
| Empirical formula | $C_{42}H_{45}N_3O_8SZn_2$ |
| $M_w$ | 882.61 |
| Crystal system | Monoclinic |
| Space group | Cc |
| Unit cell dimensions | $a$ = 17.7602(7) Å, $b$ = 16.8640(5) Å, c = 14.5089(5) Å, $\beta$ = 106.571(4) ° |
| $V$ | 4165.0(3) Å$^3$ |
| $Z$ | 4 |
| Calculated density | 1.408 Mg/m$^3$ |
| Absorption coefficient (μ) | 1.256 mm$^{-1}$ |
| Reflections (measured/ unique/observed) | 45,146/10,070/6986 |
| $R_{int}$ | 0.023 |
| Data/parameters | 10,070/542 |
| $R_1$, $wR_2$ [$I > 2\sigma(I)$] | $R_1$ = 0.0274, $wR_2$ = 0.0680 |
| $R_1$, $wR_2$ (all data) | $R_1$ = 0.0484, $wR_2$ = 0.0726 |

signals belonging to **L1** are all clearly shifted downfield upon coordination (Δδ H ~ 0.09–0.29 ppm) with the exception of those four of 3-pyridyl H atoms adjacent to the coordinated N atoms (H5/H11, Δδ H ~ 0.03 ppm; H1/H15, Δδ H ~ 0.02 ppm) which do not show significant changes. This is contrary to that expected when coordination occurs [14], the loss of electron density upon coordination to a metal usually results in shifts to lower field of the adjacent protons of the coordinated pyridyl nitrogen atoms. An explanation to this finding is that the shielding would come from the magnetic anisotropy of the π system of the chelating acac rings in the neighbourhood of these protons [14].

## 4. Conclusions

The novel terpyridine-based and potentially bridging ligand **L1** was synthesized and then characterized through spectroscopic methods. The coordinating properties of **L1** were tested by reacting with $Zn(acac)_2$ to give the dinuclear complex **1**, where **L1** acts as a bridging ligand only via its 3-pyridyl nitrogen atoms. The N atom of the central pyridine ring and the S atom of the thiomethyl unit of **L1** do not participate in the binding to the metal centres. The supramolecular structure of **1** can be understood by using the non-covalent interactions in which the thiomethyl group plays a key role through the unusual S···O and S···H contacts. These synthons act in conjunction with the abundant CH/O and CH/π hydrogen bonds to stabilize the crystal packing.

## 5. Experimental

The solvents were purchased from commercial sources and used without further purification. The compound $Zn(acac)_2$ was obtained from Aldrich. Infrared spectra were recorded using KBr plates on a Bruker Tensor 27 FT-IR spectrometer. A Exeter Analytical CE-440 elemental analyser was used for microanalysis (C, H, N). $^1$H and $^{13}$C NMR spectra were recorded on a Bruker Avance 300 MHz NMR instrument. Mass spectra were recorded on a JEOL JEM-AX505HA spectrometer by electronic impact (EI) of lower resolution at 70 eV.

### 5.1. Synthesis of 4′-(4-methylthiophenyl)-3,2′:6′,3″-terpyridine (*L1*)

The procedure of synthesis is similar to that of Hanan and Wang [15]. 3-Acetylpyridine (2.42 g, 20 mmol) was added to a solution of 4-(methylthio)benzaldehyde (1.54 g, 10 mmol) in EtOH (50 mL). KOH pellets (1.12 g, 20 mmol) were then added to the solution followed by aqueous $NH_3$ (29 mL, 25 mmol). The resulting solution was stirred at room temperature for 4 h. The solid was collected by filtration and washed with $H_2O$ (5 × 10 mL) and MeOH (3 × 10 mL). Recrystallization from $CH_2Cl_2$–MeOH afforded white solid **L1**. Yield: 1.0 g, 28%. M.p. 183–185°C. Anal. Calcd for $C_{22}H_{17}N_3S$: C, 74.34; H, 4.82; N, 11.82; S, 9.02. Found: C, 74.37; H, 4.98; N, 11.45; S, 9.20. IR (KBr, cm$^{-1}$): 3036, 2917, 1905, 1600,

1384, 808, 703 (Fig. S1). $^1$H NMR (200 MHz, $CDCl_3$, 298 K): $\delta$ = 9.29 (br d, 2H, $J$ = 1.6 Hz), 8.63 (dd, 2H, $J$ = 4.7, 1.2 Hz), 8.39 (dt, 2H, $J$ = 8.1, 1.7 Hz), 7.79 (s, 2H), AA′BB′ system observed at 7.57 (d, 2H, 8.6 Hz) and 7.30 (d, 2H, $J$ = 8.6 Hz), 7.36 (dd, 2H, $J$ = 7.9, 4.7), 2.48 (s, 3H) (Fig. S2). $^{13}$C-PND and $^{13}$C-DEPT NMR (50 MHz, $CDCl_3$, 298 K): 155.00 (2C, $C_{quat.}$), 149.95 (2C, CH), 149.69 (1C, $C_{quat.}$), 148.13 (2C, CH), 140.76 (1C, $C_{quat.}$), 134.22 (2C, CH), 134.00 (3C, $C_{quat.}$), 127.10 (2C, CH), 126.34 (2C, CH), 123.38 (2C, CH), 116.83 (2C, CH), 15.13 (1C, $CH_3$) (Fig. S3). HRMS ($FAB^+$) Calcd for $C_{22}H_{17}N_3S$ $[M + 1]^+$ 356.1221, found 356.1219, MS ($EI^+$, 70 eV) for $C_{22}H_{17}N_3S$ ($[M]^+$) 355 (100%), 354 (16.7%), 339 (7.2%), 308 (6.3%), 340 (5.7%) (Fig. S4).

### 5.2. Synthesis of [$Zn_2$($\mu$-**L1**)(acac)$_4$] (**1**)

To a hot solution (using an oil bath at 64–68 °C) of **L1** (30.0 mg, 0.084 mmol) in MeCN (15 mL) contained in a closed volumetric flask (25 mL) was added an excess of $Zn(acac)_2$ (442.8 mg, 1.680 mmol). The resultant solution was heated in the oil bath for 26 h. Block-like colourless crystals (suitable for single crystal X-ray analysis) were obtained after the removal of the hot solvent, washing with MeCN (5 × 5 mL) and diethyl ether (2 × 4 mL). Yield: 60 mg, 80.5%. Anal. Calcd for $C_{42}H_{45}N_3O_8SZn_2$: C, 57.15; H, 5.14; N, 4.76; S, 3.63. Found: C, 57.38, H, 5.32, N: 4.54, S: 3.78. IR (KBr, $cm^{-1}$): 3078, 2915, 1582, 1514, 1383, 1014, 817, 406 (Fig. S5). $^1$H NMR (300 MHz, $CDCl_3$, 298 K): $\delta$ = 9.32 (2H, dd, $J$ = 1.8, 1.5 Hz), 8.68 (2H, dt, $J$ = 8.1, 1.8 Hz), 8.65 (2H, dd, $J$ = 5.1, 1.5 Hz), 7.94 (2H, s), 7.66 (2H, d, $J$ = 6.9 Hz) 7.57 (2H, dd, $J$ = 8.1, 5.1 Hz), 7.40 (2H, d, $J$ = 6.9 Hz), 5.40 (4H, s), 2.57 (3H, s), 2.04 (24H, s) (Fig. S6). $^{13}$C-PND and $^{13}$C-DEPT-135 NMR (75 MHz, $CDCl_3$, 298 K): 193.67 (8C, $C_{quat.}$), 154.27 (2C, $C_{quat.}$), 150.49 (1C, $C_{quat.}$), 149.47 (2C, CH), 147.82 (2C, CH), 141.48 (1C, $C_{quat.}$), 136.64 (2C, CH), 135.43 (2C, $C_{quat.}$), 133.85 (1C, $C_{quat.}$), 127.23 (2C, CH), 126.63 (2C, CH), 124.52 (2C, CH), 117.48 (2C, CH), 100.01 (4C, CH), 28.26 (8C, $CH_3$), 15.31 (1C, $CH_3$) (Fig. S7).

### 5.3. X-ray crystallography

Crystal data were collected on a Oxford Gemini CCD S Ultra diffractometer at room temperature using Mo Kα radiation ($\lambda$ = 0.71073 Å). The structure was solved by direct methods and refined by full-matrix least squares on $F^2$ using the SHELXS-97 software [16]. All non-hydrogen atoms were refined anisotropically. Hydrogen atoms were found in a difference Fourier but further idealized. The structural analysis was performed with the help of the multipurpose PLATON program [17].

Data collection and refinement parameters are summarized in Table 2. The molecular representations shown in the figures were generated using XP in the SHELXTL package [16] and VESTA [18]. Crystallographic data (excluding structure factors) for the structures in this paper have been deposited with the Cambridge Crystallographic Data Centre as supplementary publication No. CCDC 838813. Copies of the data can be obtained, free of charge, on application to CCDC, 12 Union Road, Cambridge CB2 1EZ, UK, (fax: +44 1223 336033 or e-mail: deposit@ccdc.cam.ac.uk).

## Acknowledgements

The authors acknowledge the Universidad de La Frontera (Proyecto DIUFRO No. DI11-0026) for financial support. We also acknowledge the ANPCyT (Project No. PME 01113) for the purchase of the CCD diffractometer and the Spanish Research Council (CSIC) for providing a free-of charge license to the Cambridge Structural Database (Allen, 2002).

## Appendix A. Supplementary material

Supplementary data associated with this article can be found, in the online version, at doi:10.1016/j.molstruc.2011.10.038.

## References

[1] E.C. Constable, Chem. Soc. Rev. 36 (2007) 246–253.
[2] I. Eryazici, Ch.N. Moorefield, G.R. Newkome, Chem. Rev. 108 (2008) 1834–1895.
[3] (a) L. Hou, D. Li, Inorg. Chem. Commun. 8 (2005) 190;
(b) X.-Z. Li, M. Li, Z. Li, J.-Z. Hou, X.-C. Huang, D. Li, Angew. Chem. Int. Ed. 47 (2008) 6371;
(c) E.C. Constable, G. Zhang, C.E. Housecroft, M. Neuburger, J.A. Zampese, CrystEngComm 11 (2009) 2279;
(d) E.C. Constable, G. Zhang, E. Coronado, C.E. Housecroft, M. Neuburger, CrystEngComm 12 (2010) 2139.
[4] (a) J. Granifo, M. Vargas, M.T. Garland, A. Ibañez, R. Gaviño, R. Baggio, Inorg. Chem. Commun. 11 (2008) 1388;
(b) C. Liu, Y.-B. Ding, X.-H. Shi, D. Zhang, M.-H. Hu, Y.-G. Yin, D. Li, Cryst. Growth Des. 9 (2009) 1275.
[5] H. Suezawa, T. Yoshida, Y. Umezawa, S. Tsuboyama, M. Nishio, Eur. J. Inorg. Chem. (2002) 3148.
[6] (a) T. Steiner, Angew. Chem. Int. Ed. 41 (2002) 48;
(b) G.R. Desiraju, Acc. Chem. Res. 29 (1996) 441;
T. Steiner, Chem. Commun. (1997) 727.
[7] M.K. Milčič, V.B. Medaković, D.N. Sredojević, N.O. Juranić, S.D. Zarić, Inorg. Chem. 45 (2006) 4755.
[8] E. Medlycott, G.S. Hanan, Chem. Soc. Rev. 34 (2005) 133.
[9] R.E. Rosenfield Jr., R. Patthasarathy, J.D. Dunitz, J. Am. Chem. Soc. 99 (1977) 4860.
[10] M. Iwaoka, S. Takemoto, S. Tomoda, J. Am. Chem. Soc. 124 (2002) 10613.
[11] J.-A. van den Berg, K.R. Seddon, Cryst. Growth Des. 3 (2003) 643.
[12] A. Esparza-Ruiz, A. Pena-Hueso, J. Hernandez-Diaz, A. Flores-Parra, R. Contreras, Cryst. Growth Des. 7 (2007) 2031.
[13] R. Dubey, A.K. Tewari, K. Ravikumar, B. Sriddhar, Bull. Korean Chem. Soc. 31 (2010) 1326.
[14] C. Bazzicalupi, A. Bencini, A. Bianchi, A. Danesi, E. Faggi, C. Giorgi, S. Santarelli, B. Valtancoli, Coord. Chem. Rev. 252 (2008) 1052.
[15] G.R. Hanan, J. Wang, Synlett 8 (2005) 1251.
[16] G.M. Sheldrick, Acta Crystallogr., A 64 (2008) 112–122.
[17] A.L. Spek, PLATON, A Multipurpose Crystallographic Tool, Utrecht University, Utrecht, The Netherlands, 2005.
[18] K. Momma, F. Izumi, J. Appl. Crystallogr. 41 (2008) 653–658.